View metadata, citation and similar papers at core.ac.uk

brought to you by CORE

provided by Elsevier - Publisher Connector

Water Alignment, Dipolar Interactions, and Multiple Proton Occupancy during Water-Wire Proton Transport

Tom Chou

Department of Biomathematics and the Institute for Pure and Applied Mathematics, Los Angeles, California

ABSTRACT A discrete multistate kinetic model for water-wire proton transport is constructed and analyzed using Monte Carlo simulations. In the model, each water molecule can be in one of three states: oxygen lone-pairs pointing leftward, pointing rightward, or protonated (H_3O^+). Specific rules for transitions among these states are defined as protons hop across successive water oxygens. Our model also includes water-channel interactions that preferentially align the water dipoles, nearest-neighbor dipolar coupling interactions, and Coulombic repulsion. Extensive Monte Carlo simulations were performed and the observed qualitative physical behaviors discussed. We find the parameters that allow the model to exhibit superlinear and sublinear current-voltage relationships, and show why alignment fields, whether generated by interactions with the pore interior or by membrane potentials, always decrease the proton current. The simulations also reveal a "lubrication" mechanism that suppresses water dipole interactions when the channel is multiply occupied by protons. This effect can account for an observed sublinear-to-superlinear transition in the current-voltage relationship.

INTRODUCTION

The transport of protons in aqueous media and across membranes is a fundamental process in chemical reactions, solvation, and pH regulation in cellular environments (Alberts et al., 1994; Grabe and Oster, 2001). Proton transport in confined geometries is also relevant for ATP synthesis (Boyer, 1997) and light transduction by bacteriorhodopsin (Lanyi, 1995). In this article, we develop a lattice model for describing proton transport in one-dimensional environments. This study is motivated by numerous measurements of proton conduction across lipid membrane channels (Akeson and Deamer, 1991; Busath et al., 1998; Cotten et al., 1999; Cukierman et al., 1997; Deamer, 1987; Eisenman et al., 1980). Experiments are typically performed using membrane-spanning gramicidin channels that are only a few Ångstroms in diameter. This geometric constraint imposes a single-file structure on the interior water molecules (Hille and Schwarz, 1978; Hladky and Haydon, 1972).

Under equal electrochemical potential gradients, conduction of protons across ion channels occurs at a rate typically an order-of-magnitude higher than that of other small ions. This supports a ''water-wire'' mechanism (Akeson and Deamer, 1991; Nagle and Morowitz, 1978; Nagle and Tristram-Nagle, 1983; Nagle, 1987), first proposed by Grotthuss (Agmon, 1995; Grotthuss, 1806). Across a water-wire, protons are shuttled across lone-pairs of water oxygens as they successively protonate the waters along the single-file chain. Since the hydrogens are indistinguishable, any one of the hydrogens in a water cluster (e.g., any of the three hydrogens on a hydronium) can hop forward along the chain to protonate the next water molecule or cluster of water molecules (compare to Fig. 1). This mechanism naturally allows much faster overall conduction of protons compared to other small ions which have to wait for the entire chain of water molecules ahead of it to fluctuate across the pore to traverse the channel.

A peculiar feature of measured current-voltage relationships is a crossover from sublinear to superlinear behavior as the pH of the reservoirs is lowered. Measurements by Eisenman et al. (1980) were carried out in symmetric solutions in the 1–3 pH range, and the results were recently reproduced by Busath et al. (1998) and Rokitskaya et al. (2002). These experiments were performed using simple, relatively featureless gramicidin A channels. One leading hypothesis is that the nonlinear proton current-voltage relationships arise from the intrinsic proton dynamics within such simple channels. Specifically, multiple proton occupancy and repulsion among protons within the channel may give rise to the observed nonlinearity (Hille and Schwarz, 1978; Phillips et al., 1999; Schumaker et al., 2001).

There have been a number of recent theoretical studies of water-wire proton conduction. Extensive simulations on the quantum dynamics of proton exchange across small water clusters in vacuum have been used to predict microscopic hopping rates between water clusters (Bala et al., 1994; Sadeghi and Cheng, 1999; Marx et al., 1999; Mavri and Berendsen, 1995; Mei et al., 1998; Sagnella et al., 1996; Schmitt and Voth, 1999). Pomès and Roux (1996) have performed classical molecular dynamics (MD) simulations on water-channel interactions, proton hopping, and water reorientation. They derive effective potentials of mean force describing the energy barriers encountered by a single proton within the pore. Since MD simulations are presently limited to only processes that occur over a few nanoseconds, none of these computational methods are efficient at probing very long-time, steady-state transport behavior. On a more macroscopic, phenomenological level, Sagnella and Voth

Submitted September 22, 2003, and accepted for publication January 28, 2004.

Address reprint requests to Tom Chou, Dept. of Biomathematics and IPAM, Los Angeles, CA 90095-1766. Tel.: 310-206-2787; E-mail: tomchou@ucla.edu.

© 2004 by the Biophysical Society

0006-3495/04/05/2827/10 $2.00

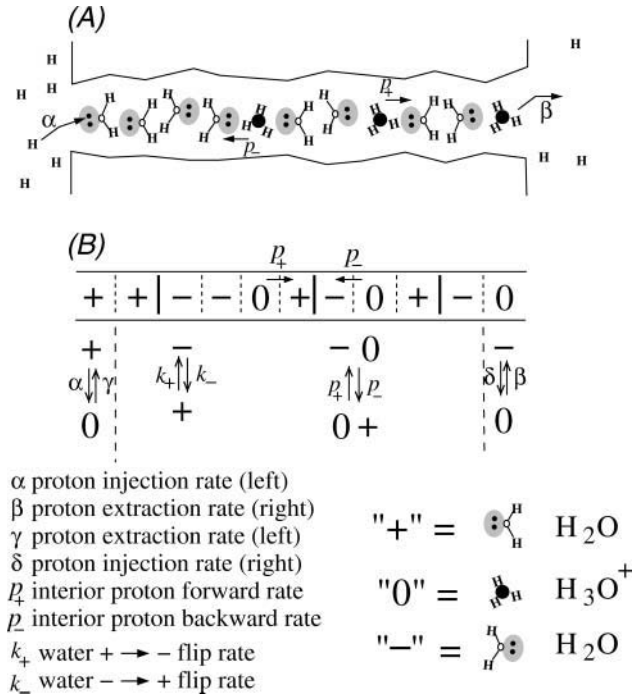

FIGURE 1 (*A*) Schematic of an $N = 11$, three-species exclusion model illustrating the steps in a Grotthuss mechanism of proton transport along a water-wire. For typical ion channels that span lipid membranes, $N \sim 10$–20. The transition rates are labeled in *B* and in the legend. Water dipole kinks are denoted by thick lines.

(1996) and Schumaker et al. (2000, 2001) have considered the long-time behavior of a single proton and dipole defect diffusing in a single-file channel. The parameters used in these studies, including effective energy profiles and kinetic rates, were derived from MD simulations. Although the basic underlying structure assumed by most of these transport models qualitatively resembles the Grotthuss mechanism, they have not addressed multiple proton occupancy. One exception are fully dynamical models that treat proton transfer in ordered water structures in the context of soliton dynamics (Bazeia et al., 2001; Pang and Feng, 2003; Pnevmatikos, 1988).

In this article, we will explore the intrinsically nonlinear proton dynamics along a single-file water-wire. We formulate a stochastic lattice model that defines the discrete structural states of the water-wire to approximate the continuous molecular orientations. Although the lattice model provides a different approach from MD simulations, it is more amenable to analysis at longer timescales, yet is connected to the microphysics inherent in MD simulations provided a consistent correspondence between the parameters is made. Rather than enumerating all possible molecular configurations, our lattice approach resembles that developed for molecular motors (Fisher and Kolomeisky, 1999), mRNA translation (MacDonald and Gibbs, 1969; Chou, 2003), traffic flow (Karimipour, 1999; Schreckenberg et al., 1995), and ion and water transport in single-file channels (Chou, 1998, 1999; Chou and Lohse, 1999). Here, the proton occupancy along the water-wire will be self-consistently determined by the prescribed lattice dynamics. The parameters used in our model are transition rates among discrete states that, in principle, can be independently computed from relatively short-time MD simulations (Dècornez et al., 1999). The approximations inherent in our discrete model qualitatively take into account the effects of proton-proton repulsion and water-water dipole interactions.

MODEL AND METHODS

Qualitatively, protons hop from oxygen to oxygen during transport. The successive hops clearly do not have to involve an individually tagged proton; in this respect, proton currents resemble electrical conduction in a conductor. Many measurements of proton conduction across membranes are performed on the gramicidin model system. The interior diameter of gramicidin A is ~3–4 Å and can only accommodate water in a single-file chain. Although the number of water molecules in this chain is a fluctuating quantity, their dynamics in and out of the channel will be assumed to be much slower than that of their orientational rearrangements and proton hopping (Hummer et al., 2001; Kalra et al., 2003). We thus treat the water-wire as containing a fixed, average number of water molecules. There are $N \approx 8$–26 single-file waters within a typical transmembrane channel (Levitt et al., 1978; Wu and Voth, 2003).

Fig. 1 *A* shows a schematic of our model. We first assume that each site along the pore is occupied by a single oxygen atom which may either be part of neutral water (H_2O), or a hydronium (H_3O^+) ion. Although protonated oxygens in bulk are often associated with larger complexes such as $H_5O_2^+$ (Zundel cation), or $H_9O_4^+$ (Eigen cation), in confined geometries, the formation of the larger complexes is suppressed (Lynden-Bell and Rasaiah, 1996). Furthermore, the model depicted in Fig. 1 *A* can incorporate the dynamics of reactive proton transfer among transient clusters by an appropriate redefinition of a lattice site to contain the entire cluster.

Neutral waters have permanent dipole moments and electron lone-pair orientations that can rotate thermally. For simplicity, we bin all water dipoles (hydrogens) that point toward the right as ''+'' particles, whereas those pointing more or less to the left are denoted ''−'' particles. The singly-protonated species H_3O^+ is hybridized to a nearly planar molecule. Therefore, we will assume that hydronium ions are symmetric with respect to transferring a proton forward or backward, provided the adjacent waters are in the proper orientation and there are no external driving forces (electric fields). Each lattice site can exist in only one of three states: 0, +, or −, corresponding to protonated, right, or left states, respectively. Labeling the occupancy configurations $\sigma_i = \{-1, 0, +1\}$, allows for fast integer computation in simulations.

In addition to proton exclusion, the transition rules are constrained by the orientation of the waters at each site and are defined in Fig. 1 *B*. A proton can enter the first site ($i = 1$) from the left reservoir and protonate the first water molecule with rate α only if the hydrogens of the first water are pointing to the right (such that its lone-pair electrons are left-pointing, ready to accept a proton). Conversely, if a proton exits from the first site back into the left reservoir (with rate γ), it leaves the remaining hydrogens right-pointing. In the pore interiors, a proton at site i can hop to the right(left) with rate $p_+(p_-)$ only if the adjacent particle is a right- (left-) pointing, unprotonated water molecule. If such a transition is made, the water molecule left at site i will be left- (right-) pointing. Physically, as a proton moves to the right, it leaves a wake of – particles to its left. A left-moving proton leaves a trail of + particles to its right. These trails of − or + particles are unable to accept another proton from the same direction. Protons can follow each other successively only if water molecules can reorient such that these trails of +'s or −'s are thermally washed out. Water reorientation rates are denoted $k_\pm$ (compare to Fig. 1 *B* and Fig. 2). Protons at the rightmost end of the water-

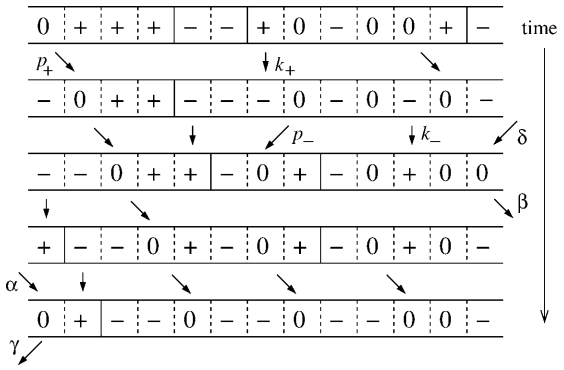

FIGURE 2 A time series depicting a number of representative transitions obeying the dynamical constraints of our model. A proton (0) at site i can move to the right with rate p_+ only if site $i + 1$ is occupied by a properly aligned (lone-pair electrons pointing to the left) water molecule (+). When a proton leaves site i to the right, it leaves behind a water in state ''−'', with lone-pair electrons pointing to the right. Protons at site i can also move to the left with rate p_- if site i–1 is a water in the ''–'' state. In this case, a water is left behind at behind site i in the ''+'' state. The neutral water molecules must flip (+ ↔ −) for a nonzero steady-state current to exist.

wire (at site $i = N$), exit with rate β, which is different from p_+ inasmuch as the local microenvironment (e.g., typical distance to acceptor electrons) of the bulk waters that accept this last proton is different from that in the pore interior. From the right reservoir, protons can hop back into the water-wire with rate δ if a water in the ''−'' configuration is at site $i = N$. The entrance rates α and δ are functions of at least the proton concentration in the respective reservoirs. Fig. 2 shows a representative time series of the evolution of a specific configuration. The rate-limiting steps in steady-state proton transfer across biological water channels are thought to be associated with water flipping (Pomès and Roux, 1998).

The lattice discretization for individual H_3O^+ ions need not be interpreted literally. Larger complexes can be effectively modeled by reinterpreting $p_\pm$, $k_\pm$, and the basic unit of hopping for the proton. For example, if certain conditions obtain, where ions are predominantly two-oxygen clusters ($H_5O_2^+$), we defined each pair of waters as occupying a single lattice site, $k_\pm$, as an effective reorientation time for the following pair of waters, and $p_\pm$ as the hopping rate to an adjacent oxygen lone-pair. The Grotthuss water-wire mechanism is qualitatively preserved as long as the proper identification with the microphysics is made.

All eight parameters used in our model (the rates $p_\pm$, $k_\pm$, α, β, γ, and δ), can be related to measured bulk quantities or derived from short-time MD simulations. They are a minimal set and are equivalent to the numerous bulk parameters used in other models (Schumaker et al., 2001), such as the bulk proton diffusion constant, water orientational diffusion constants, etc. Using similar MD approaches then, one should be able to approximately fix the parameters used in our model. For example, variations in the potential of mean force along the pore (resulting from interactions of the different species with the constituents of the pore interior) are embodied by site-dependent transition rates $p_\pm$ and $k_\pm$. Thus, MD-derived potentials of mean force used in previous models can also be implemented within our lattice framework. Such effects of local inhomogeneities in the hopping rates have been studied analytically and with MC simulations in related models (Kolomeisky, 1998).

The basic model described above has been studied analytically in certain limits where exact asymptotic results for the steady-state proton current J were derived (Chou, 2002). However, this study did not explicitly include any interactions other than proton exclusion and proton transfer onto properly aligned water dipoles. Effects arising from forces such as repulsion between protons in close proximity, interactions between water dipoles and external electric fields, and dipolar coupling between neighboring waters need to be considered.

In Fig. 3 *A*, a proton moves down the electric potential reducing the total enthalpy by V, and a right-pointing dipole is converted into a left-pointing dipole at an energy cost of H. Since both initial and final states have adjacent, repelling protons, the repulsion energy R does not enter in the overall energy change. In Fig. 3 *B*, a proton moves down the potential ($-V$), a ''+'' water is converted to a ''−'' ($+H$), a dipole domain wall is removed ($-K$), and the repulsive energy between adjacent charged protons is relieved ($-R$). The representation of these nearest-neighbor effects can be succinctly written in terms of the energy of a specific configuration,

$$E[\{\sigma_i\}] = -K\sum_{i=1}^{N-1}\sigma_i\sigma_{i+1} - H\sum_{i=1}^{N}\sigma_i + R\sum_{i=1}^{N-1}(1-\sigma_i^2) \times (1-\sigma_{i+1}^2) - V\sum_{i=1}^{N} i(1-\sigma_i^2). \quad (1)$$

The H, K, R, and V parameters used in $E[\{\sigma_i\}]$ are all in units of k_BT, and represent

- H: Energy cost for orienting a water dipole against external field.
- K: Energy cost for two oppositely oriented, adjacent dipoles.
- R: Repulsive Coulombic energy of two adjacent protons.
- V: Energy for moving a charged proton one lattice site against an external field.

V is the change in potential that a proton incurs as it moves between adjacent waters. The total transmembrane potential $V_{membrane} = NV$.

A number of microscopic details will be neglected. For example, the local dielectric environment across a channel can induce a spatially varying effective potential $V_{1\le i\le N}$ (Edwards et al., 2002; Jordan, 1984; Partenskii and Jordan, 1992; Syganow and von Kitzing, 1999). As a charge moves from the dielectric $\varepsilon \approx 80$ water phase through the $\varepsilon \approx 2$ lipid bilayer, the polarization energy varies. This smooth (on length scales over a typical water-water separation, or lattice site) energy variation ultimately gives rise

(A) . . . 0 0 + 0 . . . ⟶ . . . 0 − 0 0 . . . $\Delta E = H - V$

(B) . . . 0 0 + − . . . ⟶ . . . 0 − 0 − . . . $\Delta E = H - K - R - V$

(C) . . . + + + . . . ⟶ . . . + − + . . . $\Delta E = H + 2K$

(D) . . . 0 0 + + . . . ⟶ . . . 0 − 0 + . . . $\Delta E = H + K - R - V$

(E)

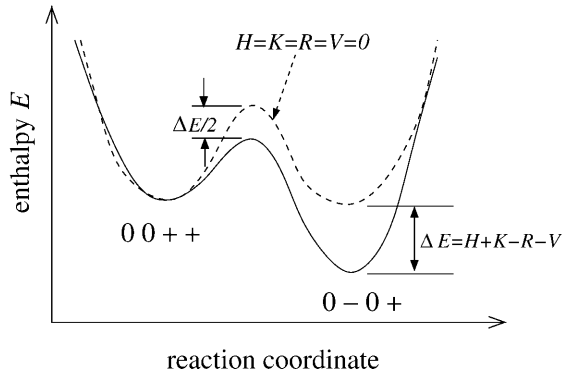

FIGURE 3 (*A–D*) Energy differences between final and initial states that involve a change in ferroelectric coupling, net dipole moment, and repulsive interactions. (*E*) A representative energy barrier profile for $H = K = R = V = 0$ (*dashed curve*). The energy profile for H, K, R, $V \neq 0$ for a transition between the states considered in *D* is shown by the thick solid curve.

to a smooth variation in the internal hopping rates, $p_{\pm}$. In this study, we neglect this variation and assume constant V and $p_{\pm}$ across the entire lattice.

More complicated interactions, such as non nearest-neighbor repulsion and interactions between protons and water dipole orientation changes have also been considered (Dellago et al., 2003). Longer-ranged electrostatic repulsion can be easily incorporated by assigning an energy for, say, next-nearest-neighbor protons. We neglect these more complicated contributions to the free energy of the system and focus on the qualitative effects of Coulomb repulsion by only considering nearest-neighbor interactions.

To connect the quantities H, K, R, and V to the rates α, β, γ, δ, $p_{\pm}$, and $k_{\pm}$, we will assume the transitions occur over thermal barriers. Although barriers to proton hopping may be small, we employ the Arrhenius forms to obtain a simple relationship so that qualitative aspects of the effects of H, K, R, and V can be illustrated. Activation energy-based treatments for conduction across gramicidin channels have been previously studied (Chernyshev and Cukierman, 2002). When the more complicated interactions and external potentials are turned on, the effective transition rates $\xi \equiv \{\alpha, \beta, \gamma, \delta, p_{\pm}, k_{\pm}\}$ on which we base our Metropolis Monte Carlo become

$$\xi = \xi_0 \exp\left(\frac{\Delta E}{2}\right), \tag{2}$$

where $\xi_0 \equiv \{\alpha_0, \beta_0, \gamma_0, \delta_0, p_0, k_0\}$ are rate prefactors when H, K, R, V, and ΔE are zero. In defining Eq. 2, we have assumed that the energy barrier due to the difference $\Delta E = E[\{\sigma_i'\}] - E[\{\sigma_i\}]$ (where $\{\sigma_i'\}$ and $\{\sigma_i\}$ are the final and initial state configurations, respectively) is evenly split between the barrier energies in the forward and backward directions. We use the convention that $p_+ = p_- = p_0$ and $k_+ = k_- = k_0$ when $V = 0$ and $H = 0$, respectively. The constraints and the state-dependent transition rates determined by Eqs. 1 and 2 completely define a nonequilibrium dynamical model which we study using MC simulations. Note that in the original model (Fig. 2) we do not assume transition barriers, but rather only that the dynamics are Markovian.

We first gain insight into the dynamics by considering numerical solutions to the full master equation for a short three-site ($N = 3$) channel. If we explicitly enumerate all $27 = 3^3$ states of the three site model, the master equation for the 27-component-state vector $\vec{P}$ is

$$\frac{d\vec{P}(t)}{dt} = \mathbf{M}\vec{P}(t), \tag{3}$$

where $\mathbf{M}$ is the transition matrix constructed from the rates ξ. In steady state, the P_i are solved by inverting $\mathbf{M}$ with the constraint $\sum_{i=1}^{27} P_i = 1$. The steady-state currents are found from the appropriate elements in P_i times the proper rate constants in the model. For example, if the probability that the three-site chain is in the configuration $(+\ -0)$ is denoted P_{12}, then the transition rate to state $P_{13} \equiv (+\ --)$ (corresponding to the ejection of a proton from the last site into the right reservoir) is βe^{V-H-K} and the steady-state current $J = \beta \Sigma_i' P_i$ (where the sum Σ_i' runs over all configurations that contain a proton at the last site), will contain the term $\beta e^{V-H-K} P_{12}$.

Monte Carlo (MC) simulations were implemented for relatively small ($N = 10$) systems by randomly choosing a site, and making an allowed transition with the probability $\xi \exp(E_i - E_f)/r_{max}$, where r_{max} is the maximum possible transition rate of the entire system. In the next time step, a particle is again chosen at random and its possible moves are evaluated. The currents were computed after the system reached steady state by counting the net transfer of protons across all interfaces (which separate adjacent sites and the reservoirs) and dividing by $N + 1$. Physical values of J are recovered by multiplying by r_{max}. Particle occupation statistics within the chain were tracked by using the definitions of $+$, 0, and $-$ particle densities at each site i: $\rho_+(i) = \langle \sigma_i(\sigma_i + 1)/2 \rangle$, $\rho_0(i) = \langle (1 - \sigma_i^2) \rangle$, and $\rho_-(i) = \langle \sigma_i(\sigma_i - 1)/2 \rangle$, respectively. However, for our subsequent discussion, it will suffice to analyze simply the chain-averaged proton concentration $\bar{\sigma}_0 = \sum_{i=1}^{N} \rho_0(i)$. All MC results were checked and compared with the exact numerical results from the three-site, 27-state master equation.

RESULTS AND DISCUSSION

We present MC simulation results for a lattice of size $N = 10$. The mechanisms responsible for the different qualitative behaviors are revealed and the effects of each interaction term will be systematically analyzed. We explore a range of relative kinetic rates, all non dimensionalized in units of p_0, the intrinsic proton hopping rate from between adjacent waters. Estimates for p_0 derived from quantum MD simulations are on the order of 1 ps^{-1} (Sadeghi and Cheng, 1999; Mavri and Berendsen, 1995; Mei et al., 1998; Schmitt and Voth, 1999). Moreover, a direct simulation of proton movement in carbon nanotube water-wires yields a proton diffusion constant of $\sim$0.1 nm^2/s (Dellago et al., 2003). With a typical interwater spacing of 0.242 nm, this diffusion constant corresponds to a hopping rate of $p_0 \sim 4$ ps^{-1}. The resulting steady-state proton currents under realistic driving forces are on the order of 10 ns^{-1}, consistent with that observed in gramicidin channels.

One of the main features we wish to explore is the effect of multiple proton occupancy on current-voltage relationships. To understand what values of transition rates would permit multiple proton occupancy, consider water at pH = 7, which has 10^{-7} M protons and hydroxyls. This concentration corresponds to $\sim$60 H_3O^+ and 60 OH^- species per cubic micron. Even at pH 4, one would only have $\sim$60,000 hydroniums per μm^3, corresponding to a typical distance between hydroniums of $\sim$25 nm. Since there are only $\sim$10–20 waters within a single-file channel, and at pH 4, only $\sim$1 in 500,000 waters are protonated in bulk, multiple protons in a single channel can occur only if protonated species within the channel are highly stabilized by interactions with the chemical subgroups comprising the pore interior. This stabilizing effect is modeled by small escape rates β_0, γ_0, and assumed to be distributed equally such that p_0 remains constant across all sites within the lattice. Although from a concentration point of view, small entrance rates α_0, δ_0 arise from infrequent protons that wander into the first site of the channel, their exit rates β_0, γ_0 can be suppressed even more by their stabilization once inside the channel. Multiple ion occupancy has also been observed in related pore systems such as the potassium channel containing three sites for K^+ ions (Morais-Cabral et al., 2001; Bernèche and Roux, 2001). Despite low bulk ion concentrations, the channel interior stabilizes the ions such that exit rates γ_0, β_0 are small enough for appreciable simultaneous multiion occupancy. In all of our simulations, we will assume proton stabilization is moderately strong and limit ourselves to the rates β_0, $\gamma_0 < \alpha_0$, δ_0. The values we use give steady-state proton occupancies across the whole range of values from $\lesssim 1$ to N.

First consider symmetric solutions and featureless, uniform pores where $\alpha_0 = \delta_0$, $\beta_0 = \gamma_0$. The only possible driving force is an external voltage V. In Fig. 4, we plot the current-voltage relationship for various flipping rates k_0. We initially ignore interaction effects and set $H = K = R = 0$.

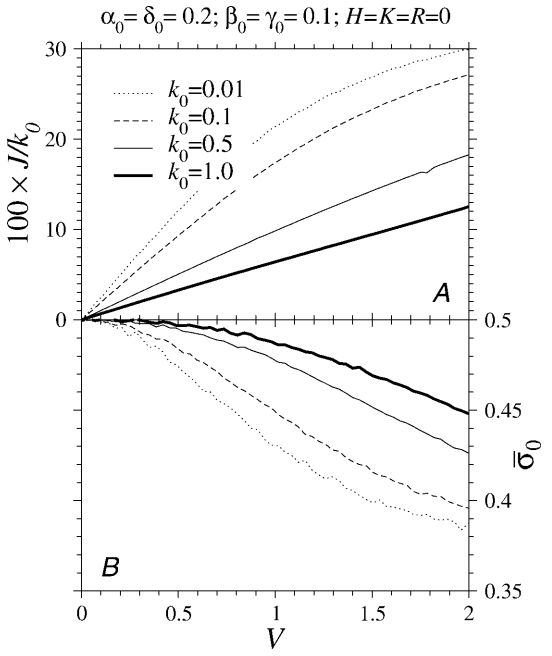

FIGURE 4 Saturation due to small flip rates $k_+ = k_- = k_0$. Currents and rates in all plots are non dimensionalized by units of p_0. (*A*) Small k_0 determines the rate-limiting step whereupon increasing V does little to increase the current. Increasing k_0 pushes the sublinear (saturation) regime of the *J–V* relationship to larger values of voltage V. (*B*) The total proton occupancy decreases with decreasing k_0.

Currents for sufficiently small V are always nearly linear. However, for sufficiently large V, the rate-limiting step eventually becomes the water-flipping rate k_0. Further increases in V do not increase the overall steady-state current, and the current-voltage curve becomes sublinear before saturating. The crossover to sublinear (water-flipping rate-limited) behavior depends on the value of k_0, with sublinear onset occurring at higher voltages V for larger k_0. In the noninteracting case, for most reasonable values of rate constants, any possible superlinear regime does not arise as it is washed out by the sublinear, water-flip rate-limited saturation. The only instance found where noticeable superlinear behavior in the steady-state proton current arises is in the limit of large k_0 and when $\alpha_0, \delta_0, p_0 \ll \beta_0, \gamma_0$. Superlinear relationships can occur via other mechanisms not inherent in our model. For example, the transmembrane potential may compress the bilayer and mechanically increasing the effective diameter of the channel, and increasing the mean number of waters in the pore. A small decrease in the interwater spacing could dramatically increase the internal hopping rate p_0, leading to a superlinear *J–V* relationship.

For the parameters explored, the currents J increase with increasing k_0 (Fig. 4 *A*); thus, the mean proton occupancies are qualitatively consistent with dynamics limited by internal proton hops. For small flipping rates, successive entry of protons is slow, whereas exit is not affected. As k_0 is increased, the bottlenecks near the entrance are relieved to a greater degree than those near the exit, increasing the overall proton occupancy (compare to Fig. 4 *B*).

Fig. 5 displays the effects of a fixed, external, dipole-orienting field $H \neq 0$. All other interactions and fields, except the external driving voltage V, are turned off. The convention used in the energy Eq. 1 favors a ''+'' state for $H > 0$. This asymmetry leads to an asymmetry in the *J–V* relationship (Fig. 5 *A*). After an initial proton has traversed the channel, flipping of the ''−'' waters left in its wake is suppressed for $H > 0$, thereby preventing further net proton movement. The persistent blockade induced by increasing H is evident in Fig. 5 *B* where the proton density decreases for increasing H.

Although H is assumed independent of V in Fig. 5, permanent water dipoles will be influenced by externally applied electric fields. The water dipoles will energetically prefer to align with this external field with a strength H proportional to V. The orientational polarizability L_{HV} is defined through $H = L_{\mathrm{HV}}V$. It has been conjectured that when L_{HV} is positive (defined as preferring waters with lone-pairs pointing to the left, or in the ''+'' state), the current should increase superlinearly with V, inasmuch as waters ahead of any proton will be oriented properly in order to receive it. Fig. 6 shows the current-voltage relationship for various L_{HV}. Although for very small L_{HV}, the current does increase very slightly, it becomes severely sublinear for larger L_{HV} and V. In fact, it can attain a negative differential resistance (NDR) similar to that found in Gunn diodes or other ''negistor'' devices. The physical origins of NDR in

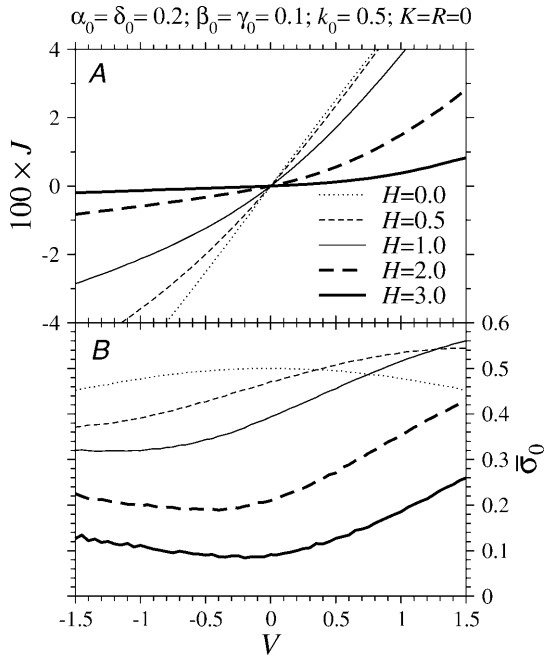

FIGURE 5 Currents (*A*) and averaged proton occupation (*B*) in the presence of a constant water dipole-aligning field $H > 0$. For larger V, the V-independent assumption for H used in this scenario will break down due to the orientation effects of V on the water dipoles.

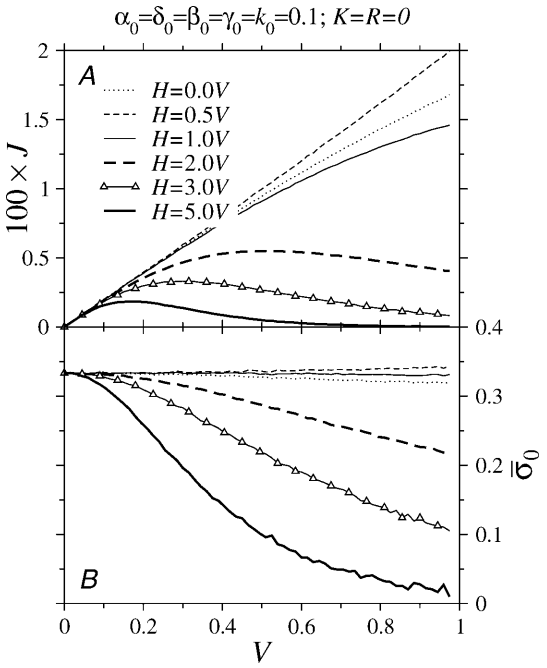

FIGURE 6 Effects of water dipole orientational polarizability ($H \equiv L_{HV}V \neq 0$). (*A*) Negative differential resistance (NDR) for large L_{HV}, V. Although transitions such as $\ldots -+0-+\ldots \rightarrow \ldots -+0++\ldots$ are accelerated, giving rise to a state where proton transport to the right is possible, NDR can arise because transitions such as $\ldots -\ +0++\ldots \rightarrow \ldots -+-0+\ldots$ created an additional ''–'' particle and is disfavored. (*B*) The average proton occupation decreases as V for large L_{HV}.

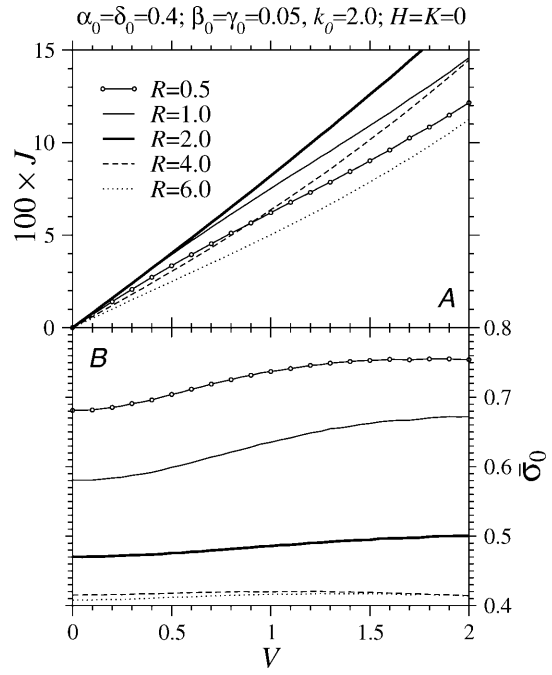

FIGURE 7 The effects of increasing nearest-neighbor proton-proton repulsion within the chain. Fixed parameters are $\alpha_0 = \delta_0 = 0.4$, $\beta_0 = \gamma_0 = 0.05$, $k_0 = 2.0$, and $H = K = 0$. (*A*) The onset of sublinear behavior in the *J–V* relationship is delayed for larger repulsions, R, making the curves appear locally more superlinear. (*B*) The average proton densities per site. For small R, although densities are high, increasing V increases the clearance rate near the entrance such that the effectively increased injection increases overall proton density. At higher repulsions, R, the clearance effect is not as strong and the simultaneously increased extraction rate prevents a large increase in the overall proton density.

proton conduction arise from the energetic cost of producing a ''−'' state as a proton moves forward. Although the path ahead of the proton is biased to ''+'' states, the proton transfer step as defined in our model necessarily leaves behind a ''−'' particle. Thus, although the field $H = L_{HV}V$ properly aligns waters ahead of a proton, it also provides an energy cost for the tail of ''−'' particles left by a forward-moving proton. This energetic penalty inhibits the proton from moving forward despite the direct driving force V acting on it.

The average density plotted in Fig. 6 *B* decreases as V for large L_{HV}. A large orientational polarizability L_{HV} not only hinders forward proton hops, but enhances backward hops of protons that have just hopped forward during its previous time step. Proton dynamics are slowed dramatically, and only at the last site can they exit the pore. Proton entry from the left reservoir, on the other hand, is often quickly followed by exit back into the left reservoir. The protons are effectively entry-limited, and the density is rather low. As V increases, the dynamics become even more entry-limited, and the overall proton occupancy decreases.

The effects of proton-proton repulsion ($R > 0$) are considered in Figs. 7 and 8. These simulations are consistent with the hypothesis that proton-proton repulsions can give rise to superlinear current (Hille and Schwarz, 1978). Fig. 7 *A* shows a slight preference for superlinear behavior as repulsion R is increased. Not surprisingly, Fig. 7 *B* shows that the overall density of protons within the pore decreases with increasing repulsion.

The sublinear-to-superlinear behavior as the proton concentration in the identical reservoirs is increased is shown in Fig. 8 *A*. Although for these parameters the effect is not striking, there is indeed a trend away from sublinear behavior as pH is decreased or as $\alpha_0 = \delta_0$ is increased. Measurements, however, also show rather modest superlinear behavior (Eisenman et al., 1980; Phillips et al., 1999; Rokitskaya et al., 2002). The occupancy also increases with decreasing pH, enhancing the effect of proton-proton repulsion. These behaviors are consistent with experimental findings (Eisenman et al., 1980) and those in the simulations depicted in Fig. 7, where increased repulsion exhibited superlinear *J–V* curves.

Finally, we consider the effects of dipole coupling $K \neq 0$ between adjacent water molecules. This interaction is analogous to a nearest-neighbor ferromagnetic coupling in e.g., Ising models. Fig. 9 *A* shows that for sufficiently large $\alpha_0 = \delta_0$, a superlinear behavior arises (for small enough V and large enough k_0 such that saturation has not yet occurred). Notice that as $\alpha_0 = \delta_0$ is increased, the *J–V*

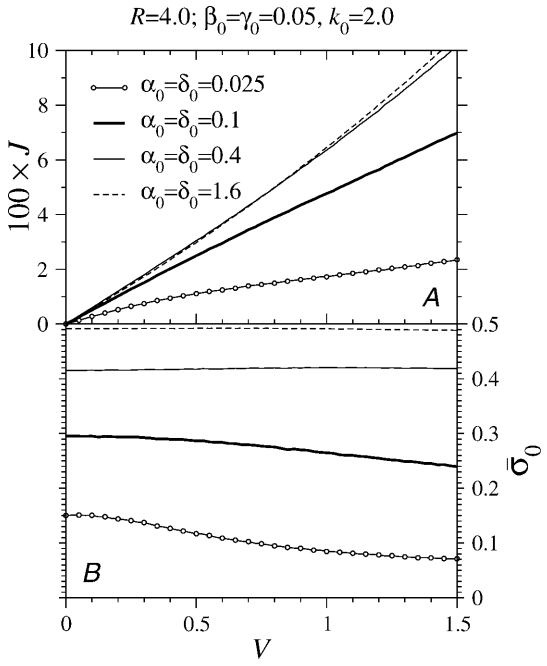

FIGURE 8 Transition from sublinear to superlinear current behavior as proton concentration in the symmetric reservoirs is increased. (*A*) *J–V* relationship for various concentrations $\alpha_0 = \delta_0$ for fixed $H = K = 0, R = 4.0$, $\beta_0 = \gamma_0 = 0.05$, and $k_0 = 2.0$. (*B*) The averaged proton concentration σ_0 at each lattice site as a function of driving voltage. The concentrations increase for all ranges of V as $\alpha = \delta$ is increased.

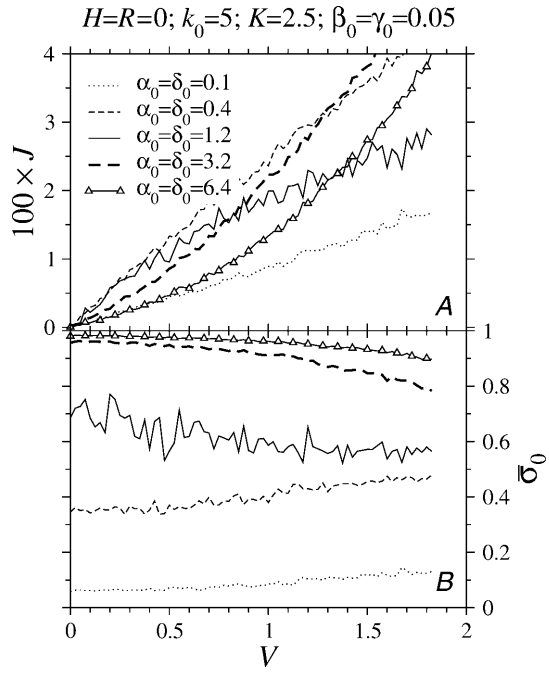

FIGURE 9 (*A*) The current-voltage relationship for various proton injection rates in the presence of ferromagnetic water dipole coupling. (*B*) Mean proton occupations increase with increasing injection rates.

relationship can become more sublinear before turning superlinear. Here we have used a higher value of k_0 to suppress sublinear behavior to larger V, but the qualitative shift from sublinear to slightly superlinear behavior exists for small k_0. Moreover, recent comparisons between gramicidin A and gramicidin M channels suggest that water reorientation is not rate-limiting (Gowen et al., 2002). The nature of the superlinear behavior can be deduced from Fig. 9 *B*, where the mean proton density is shown to increase with $\alpha_0 = \delta_0$. Waters that neighbor a proton are relieved of their dipolar coupling and can more readily flip to a configuration that would allow acceptance of another proton. For example, the transition $\ldots 0 - 0 \ldots \rightarrow \ldots 0 + 0 \ldots$ will occur faster than $\ldots - \; -0 \ldots \rightarrow \ldots - + 0 \ldots$. This lubrication effect arises only when the proton density is high and $K \neq 0$.

SUMMARY AND CONCLUSIONS

We have developed a lattice model for proton conduction that quantifies the kinetics among three approximate states of the individual water molecules inside a simple, single-file channel such as gramicidin A. The three states represent water molecules with left- and right-pointing water dipoles, and protonated ions. Our approach allows us to explore the steady-state behavior of proton currents, occurring over timescales inaccessible by MD simulations. Our theory, along with analyses of Monte Carlo simulations, extend analytic models (Schumaker et al., 2000, 2001) to include multiple proton occupancy and the memory effects of protons that have recently traversed the water-wire. Monte Carlo simulations of the lattice model were performed to test conjectures on a number of observed qualitative features in proton transport across water-wires. Four interaction energies that modify the kinetic rates are considered: A dipole-orienting field, which tends to align the water molecules; a ferromagnetic dipole-dipole interaction between neighboring water molecules; a penalty from the repulsion between neighboring protons; and an external electric field (transmembrane potential) that biases the hops of the charged protons.

We find current-voltage relationships that can be both superlinear and sublinear depending on the voltage V. For large enough voltages, the proton-hopping step is no longer rate-limiting. Water-flipping rates limit proton transfer and further increases in V do little to increase the steady-state proton current J. This observation suggests that the observed transition from sublinear to superlinear behavior can be effected by varying an effective water-flipping rate, although we find that, indeed, proton-proton repulsion can lead to slightly superlinear *J–V* characteristics—particularly for large repulsions and proton injection rates (low pH).

Dipole-dipole interactions between neighboring waters are also incorporated. Previous single-proton theories (Schumaker et al., 2000, 2001) have considered the propagation of a single defect back and forth in the pore. In our model, the number of protons and defects are dynamical variables that

depend on the injection rates and the dipole-dipole coupling, respectively. For large coupling K, we expect very few defects, and effective water-flipping rates will be low. However, when injection rates and proton occupancy in the pore is high, some dipole-dipole couplings are broken up by the intervening protons. Thus, protons can ''lubricate'' their neighboring dipoles, allowing them to flip faster than if they were neighboring a dipole pointed in the same direction. Using simulations, we showed that this lubrication effect can give rise to a superlinear J–V relationship.

The parameters used in our analyses can be estimated from shorter time MD simulations, or other continuum approximations (Dècornez et al., 1999); Edwards et al., 2002; Partenskii and Jordan, 1992). More complicated local interactions with membrane lipid dipoles (Rokitskaya et al., 2002) and internal pore constituents (such as Trp side groups; Dorigo et al., 1999; Gowen et al., 2002) can be incorporated by allowing H, K, p_0, and/or k_0 to reflect the local molecular environment by varying along the lattice site (position) within the channel (Kolomeisky, 1998).

APPENDIX: NONINTERACTING MEAN-FIELD RESULTS

For the sake of completeness, and as a qualitative guide, we review analytic results in the case $R = K = H = 0$, where only exclusions are included. Some of these results have been derived previously using mean-field approximations (Chou, 2002).

If $V = 0$ ($\xi = \xi_0$), only pH differences between the two reservoirs can induce a nonzero steady-state proton current. The proton concentration difference is reflected by a difference between the entry rates from the two reservoirs $\alpha_0 \neq \delta_0$, and the steady-state current can be expanded in powers of $1/N$: $J = a_1/N + a_2/N^2 + \mathcal{O}(N^{-3})$. In the long chain limit, we found (Chou, 2002)

$$J \sim \frac{k_+k_-}{N(k_+ + k_-)} \times \ln\left[\frac{\beta(k_+ + k_-) + k_+\delta}{\gamma(k_- + k_+) + k_-\alpha}\,\frac{\gamma(k_+ + k_-) + \alpha(p_- + k_-)}{\beta(k_+ + k_-) + k_+\delta(p_-/k_- + 1)}\right] + \mathcal{O}(N^{-2}). \quad \text{(A1)}$$

For channels with reflection-symmetric molecular structures, $\beta_0 = \gamma_0$; and Eq. A1 can be further simplified by expanding in powers of $k_-\alpha - k_+\delta$,

$$J \sim \frac{\beta p_+k_-(k_-\alpha - k_+\delta)}{N[\beta(k_- + k_+) + k_+\delta](\beta + \delta)(k_+ + k_-)} + O\big((k_-\alpha - k_+\delta)^2\big) + \mathcal{O}(1/N^2). \quad \text{(A2)}$$

Finally, in the large α and $\delta = 0$ limit,

$$J \sim \frac{k_+k_-}{(k_+ + k_-)N}\log\left(1 + \frac{p_-}{k_+}\right) - \frac{\gamma k_+k_-p_-}{\alpha N(k_+ + k_-)(k_+ + p_-)} + \mathcal{O}(\alpha^{-2}N^{-1}). \quad \text{(A3)}$$

For driven systems, where, say, $\alpha > \delta$, $\beta > \gamma$, and $p_+ > p_-$, a finite current persists in the $N \to \infty$ limit. We can use mean-field approximations familiar in the totally asymmetric simple exclusion process (TASEP) (Derrida, 1998; Schütz and Domany, 1993) to conjecture that three current regimes exist. If the both proton entry and exit is fast, and the rate-limiting steps involve water flipping, or interior protons hops with rate p_+, we expect that a maximal current regime exists and that the densities of the three states along the interior of a long chain are spatially uniform. Mean-field analysis from previous work (Chou, 2002) yields

$$J = \frac{2(p_+k_- - p_-k_+)}{(p_+ + p_-)^2}\left[\frac{(p_- + p_+)}{2} + k_- + k_+ - \sqrt{k_+ + k_-}\sqrt{k_- + k_+ + p_+ + p_-}\right]. \quad \text{(A4)}$$

For a purely asymmetric process, $p_- = 0$, and the current approaches the analogous maximal-current expression of the single species TASEP,

$$J(p_- = 0) \sim \frac{p_+k_-}{4(k_- + k_+)} + \mathcal{O}\left(\frac{p_+}{k_-}\right), \quad \text{(A5)}$$

except for the additional factor of $k_-/(k_- + k_+)$ representing the approximate fraction of time sites ahead of a proton in the ''+'' configuration. These approximations neglect the influence of protons that have recently passed, temporarily biasing the water to be in a ''−'' configuration. Therefore, it is not surprising that these results are accurate only in the $k_+, k_- \gg p$ limit.

A similar approach is taken when the currents are entry- or exit-limited. From the mean-field approximation of the steady-state equation for $\rho_\pm$ near the channel entry,

$$\frac{\partial\rho_-}{\partial t} = p_+\rho_0\rho_+ + k_+\rho_+ - k_-\rho_- = 0$$
$$\frac{\partial\rho_+}{\partial t} = -\alpha\rho_+ - k_+\rho_+ + k_-\rho_- = 0, \quad \text{(A6)}$$

where we have for simplicity set $p_- = \gamma = 0$. Upon using normalization $\rho_- + \rho_0 + \rho_+ = 1$, and the expressions in Eq. A6, we find the mean densities near the left boundary,

$$\rho_- = \frac{(\alpha + k_-)(p_+ - \alpha)}{p_+(\alpha + k_- + k_+)}, \quad \rho_+ = \frac{k_-(p - \alpha)}{p_+(\alpha + k_- + k_+)}, \quad \text{(A7)}$$

and the approximate entry-rate-limited steady-state current,

$$J \approx p_+\rho_0\rho_+ = \alpha\rho_+ = \frac{\alpha k_-(1 - \alpha/p)}{(\alpha + k_- + k_+)}. \quad \text{(A8)}$$

This result resembles the steady-state current of the low density phase in the simple exclusion process (Derrida, 1998; Chou, 2003), except for the factor $k_-/(\alpha + k_- + k_+)$, representing the fraction of time the first site is in the ''+'' state, and able to accept a proton from the left reservoir.

When the rate β is rate-limiting, we consider the mean-field equations near the exit of the channel

$$\frac{\partial\rho_-}{\partial t} = \beta\rho_0 + k_+\rho_+ - k_-\rho_- = 0$$
$$\frac{\partial\rho_+}{\partial t} = -p_+\rho_0\rho_+ + k_-\rho_- - k_+\rho_+ = 0, \quad \text{(A9)}$$

and their solutions

$$\rho_- = \frac{\beta(k_+ + p_+ - \beta)}{p_+(k_- + \beta)}, \quad \rho_+ = \frac{\beta}{p_+}. \tag{A10}$$

The exit-limited steady-state current is thus

$$J \approx \beta\rho_0 = \frac{\beta}{k_- + \beta}\left(k_- - \frac{\beta(k_- + k_+)}{p_+}\right). \tag{A11}$$

The results above are derived from mean-field assumptions which neglect correlations in particle occupancy between neighboring sites. Although mean-field theory happens to give exact results for the simple exclusion process, the results above are only exact in the large $k_\pm/p_\pm$ limit, as has been shown by Monte Carlo simulations (Chou, 2002). Only in this limit, where the memory of a previously passing proton is quickly erased, are the mean-field results quantitatively accurate (Chou, 2002). Nonetheless, the mean-field calculations of the simplified system ($H = K = R = 0$) yields qualitatively correct results for the steady-state current, provides a connection with well-known results of the TASEP, and gives an explicit qualitative description of the mechanisms at play.

The author thanks M. Schumaker for vital discussions and comments on the manuscript.

This work was performed with the support of the National Science Foundation through grant DMS-0206733.

REFERENCES

Agmon, N. 1995. The Grotthuss mechanism. *Chem. Phys. Lett.* 244: 456–462.

Alberts, B., D. Bray, J. Lewis, M. Raff, K. Roberts, and J. D. Watson. 1994. Molecular Biology of the Cell. Garland Publishing, New York.

Akeson, M., and D. W. Deamer. 1991. Proton conductance by the gramicidin water-wire: model for proton conductance in the F1F0 ATPases? *Biophys. J.* 60:101–109.

Bala, P., B. Lesyng, and J. A. McCammon. 1994. Applications of quantum-classical and quantum-stochastic molecular dynamics for proton transfer processes. *Chem. Phys.* 180:271–285.

Bazeia, D., V. B. P. Leite, B. H. B. Lima, and F. Morales. 2001. Soliton model for proton conductivity in Langmuir films. *Chem. Phys. Lett.* 340:205–210.

Bernèche, S., and B. Roux. 2001. Energetics of ion conduction through the K^+ channel. *Nature.* 414:73–77.

Boyer, P. 1997. The ATP synthase—a splendid molecular machine. *Annu. Rev. Biochem.* 66:717–749.

Busath, D. D., C. D. Thulin, R. W. Hendershot, L. R. Phillips, P. Maughn, C. D. Cole, N. C. Bingham, S. Morrison, L. C. Baird, R. J. Hendershot, M. Cotten, and T. A. Cross. 1998. Non-contact dipole effects on channel permeation. I. Experiments with (5F-indole)Trp-13 gramicidin A channels. *Biophys. J.* 75:2830–2844.

Chernyshev, A., and S. Cukierman. 2002. Thermodynamic view of activation energies of proton transfer in various gramicidin A channels. *Biophys. J.* 82:182–192.

Chou, T. 1998. How fast do fluids squeeze through microscopic single-file channels? *Phys. Rev. Lett.* 80:85–89.

Chou, T. 1999. Kinetics and thermodynamics across single-file pores: solute permeability and rectified osmosis. *J. Chem. Phys.* 110:606–615.

Chou, T., and D. Lohse. 1999. Entropy-driven pumping in zeolites and ion channels. *Phys. Rev. Lett.* 82:3552–3555.

Chou, T. 2002. A spin flip model for one-dimensional water-wire proton transport. *J. Phys. Chem. A.* 35:4515–4526.

Chou, T. 2003. Ribosome recycling, diffusion, and mRNA loop formation in translational regulation. *Biophys. J.* 85:755–773.

Cotten, M., C. Tian, D. D. Busath, R. B. Shirts, and T. A. Cross. 1999. Modulating dipoles for structure-function correlations in the gramicidin A channel. *Biochemistry.* 38:9185–9197.

Cukierman, S., E. P. Quigley, and D. S. Crumrine. 1997. Proton conductance in gramicidin A and its dioxolane-linked dimer in different bilayers. *Biophys. J.* 73:2489–2502.

Deamer, D. W. 1987. Proton permeation of lipid bilayers. *J. Bioenerg. Biomembr.* 19:457–479.

Dècornez, H., K. Drukker, and S. Hammes-Schiffer. 1999. Solvation and hydrogen-bonding effects on proton wires. *J. Phys. Chem. A.* 103:2891–2898.

Derrida, B. 1998. An exactly soluble non-equilibrium system: the asymmetric simple exclusion process. *Phys. Rep.* 301:65–83.

Dellago, C., M. M. Naor, and G. Hummer. 2003. Proton transport through water-filled carbon nanotubes. *Phys. Rev. Lett.* 90:105902.

Dorigo, A. E., D. G. Anderson, and D. D. Busath. 1999. Noncontact dipole effects on channel permeation. II. Trp conformations and dipole potentials in gramicidin A. *Biophys. J.* 76:1897–1908.

Edwards, S., B. Corry, S. Kuyucak, and S.-H. Chung. 2002. Continuum electrostatics fails to describe ion permeation in the gramicidin channel. *Biophys. J.* 83:1348–1360.

Eisenman, G., B. Enos, J. Hägglund, and J. Sandblom. 1980. Gramicidin as an example of a single-filing ionic channel. *Ann. N. Y. Acad. Sci.* 339:8–20.

Fisher, M. E., and A. B. Kolomeisky. 1999. The force exerted by a molecular motor. *Proc. Natl. Acad. Sci. USA.* 96:6597–6602.

Grabe, M., and G. Oster. 2001. Regulation of organelle acidity. *J. Gen. Physiol.* 117:329–343.

Gowen, J. A., J. C. Markham, S. E. Morrison, T. A. Cross, D. A. Busath, E. J. Mapes, and M. F. Schumaker. 2002. The role of Trp side chains in tuning single proton conduction through gramicidin channels. *Biophys. J.* 83:880–898.

Grotthuss, C. J. T. 1806. Sur la décomposition de l'eau et des corps qu'elle tient en dissolution á l'aide de l'électricité galvanique, *Ann. Chim.* 58:54–74.

Hille, B., and W. Schwarz. 1978. Potassium channels as multi-ion single-file pores. *J. Gen. Physiol.* 72:409–442.

Hladky, S. B., and D. A. Haydon. 1972. Ion transfer across lipid membranes in the presence of gramicidin A. I. Studies of the unit conductance channel. *Biochim. Biophys. Acta.* 274:294–312.

Hummer, G., J. C. Rasaiah, and J. P. Noworyta. 2001. Water conduction through the hydrophobic channel of a carbon nanotube. *Nature.* 414:188–190.

Jordan, P. C. 1984. The total electrostatic potential in a gramicidin channel. *J. Membr. Biol.* 78:91–102.

Kalra, A., S. Garde, and G. Hummer. 2003. Osmotic water transport through carbon nanotube membranes. *Proc. Natl. Acad. Sci. USA.* 100:10175–10180.

Karimipour, V. 1999. Multispecies asymmetric simple exclusion process and its relation to traffic flow. *Phys. Rev. E.* 59:205–212.

Kolomeisky, A. B. 1998. Asymmetric simple exclusion model with local inhomogeneity. *J. Phys. A Math. Gen.* 31:1153–1164.

Lanyi, J. K. 1995. Bacteriorhodopsin as a model for proton pumps. *Nature.* 375:461–463.

Levitt, D. G., S. R. Elias, and J. M. Hautman. 1978. Number of water molecules coupled to the transport of sodium, potassium and hydrogen ions via gramicidin, nonactin or valinomycin. *Biochim. Biophys. Acta.* 512:436–451.

Lynden-Bell, R. M., and J. C. Rasaiah. 1996. Mobility and solvation of ions in channels. *J. Chem. Phys.* 105:9266–9280.

MacDonald, C. T., and J. H. Gibbs. 1969. Concerning the kinetics of polypeptide synthesis on polyribosomes. *Biopolymers.* 7:707–725.

Marx, D., M. E. Tuckerman, J. Hutter, and M. Parrinello. 1999. The nature of the hydrated excess proton in water. *Nature*. 397:601–604.

Mavri, J., and H. J. C. Berendsen. 1995. Calculation of the proton transfer rate using density matrix evolution and molecular dynamics simulations: inclusion of the proton excited states. *J. Phys. Chem.* 99:12711–12717.

Mei, H. S., M. E. Tuckerman, D. E. Sagnell, and M. L. Klein. 1998. Quantum nuclear ab initio molecular dynamics study of water-wires. *J. Phys. Chem. B*. 102:10446–10458.

Morais-Cabral, J. H., Y. Zhou, and R. MacKinnon. 2001. Energetic optimization of ion conduction rate by the K+ selectivity filter. *Nature*. 414:37–42.

Nagle, J. F. 1987. Theory of passive proton conductance in lipid bilayers. *J. Bioenerg. Biomembr.* 19:413–426.

Nagle, J. F., and H. J. Morowitz. 1978. Molecular mechanisms for proton transport in membranes. *Proc. Natl. Acad. Sci. USA*. 75:298–302.

Nagle, J. F., and S. Tristram-Nagle. 1983. Hydrogen bonded chain mechanisms for proton conduction and proton pumping. *J. Membr. Biol.* 74:1–14.

Pang, X. F., and Y. P. Feng. 2003. Mobility and conductivity of the proton transfer in hydrogen-bonded molecular systems. *Chem. Phys. Lett.* 373:392–401.

Partenskii, M. B., and P. C. Jordan. 1992. Nonlinear dielectric behavior of water in transmembrane ion channels: ion energy barriers and the channel dielectric constant. *J. Chem. Phys.* 96:3906–3910.

Phillips, L. R., C. D. Cole, R. J. Hendershot, M. Cotten, T. A. Cross, and D. D. Busath. 1999. Noncontact dipole effects on channel permeation. III. Anomalous proton conductance effects in gramicidin. *Biophys. J.* 77: 2492–2501.

Pnevmatikos, S. 1988. Soliton dynamics of hydrogen-bonded networks: a mechanism for proton conductivity. *Phys. Rev. Lett.* 60:1534–1537.

Pomès, R., and B. Roux. 1996. Structure and dynamics of a proton wire: a theoretical study of H^+ translocation along the single-file water chain in the gramicidin A channel. *Biophys. J.* 71:19–39.

Pomès, R., and B. Roux. 1998. Free energy profiles for H^+ conduction along hydrogen-bonded chains of water molecules. *Biophys. J.* 75:33–40.

Rokitskaya, T. I., E. A. Kotova, and Y. N. Antonenko. 2002. Membrane dipole potential modulates proton conductance through gramicidin channel: movement of negative ionic defects inside the channel. *Biophys. J.* 82:865–873.

Sadeghi, R. R., and H.-P. Cheng. 1999. The dynamics of proton transfer in a water chain. *J. Chem. Phys.* 111:2086–2094.

Sagnella, D. E., K. Laasonen, and M. L. Klein. 1996. Ab initio molecular dynamics study of proton transfer in a polyglycine analog of the ion channel gramicidin A. *Biophys. J.* 71:1172–1178.

Sagnella, D. E., and G. A. Voth. 1996. Structure and dynamics of hydronium in the ion channel gramicidin A. *Biophys. J.* 70:2043–2051.

Schmitt, U. W., and G. A. Voth. 1999. The computer simulation of proton transport in water. *J. Chem. Phys.* 111:9361–9381.

Schreckenberg, M., A. Schadschneider, K. Nagel, and N. Ito. 1995. Discrete stochastic models for traffic flow. *Phys. Rev. E.* 51:2939–2949.

Schumaker, M. F., R. Pomès, and B. Roux. 2000. A combined molecular dynamics and diffusion model of single-proton conduction through gramicidin. *Biophys. J.* 78:2840–2857.

Schumaker, M. F., R. Pomès, and B. Roux. 2001. Framework model for single proton conduction through gramicidin. *Biophys. J.* 80:12–30.

Schütz, G., and E. Domany. 1993. Phase transitions in an exactly soluble one-dimensional exclusion process. *J. Stat. Phys.* 72:277–296.

Syganow, A., and E. von Kitzing. 1999. (In)validity of the constant field and constant currents assumptions in theories of ion transport. *Biophys. J.* 76:768–781.

Wu, Y., and G. A. Voth. 2003. A computer simulation study of the hydrated proton in a synthetic proton channel. *Biophys. J.* 85:864–875.